Since January 2020 Elsevier has created a COVID-19 resource centre with free information in English and Mandarin on the novel coronavirus COVID-19. The COVID-19 resource centre is hosted on Elsevier Connect, the company's public news and information website.

Elsevier hereby grants permission to make all its COVID-19-related research that is available on the COVID-19 resource centre - including this research content - immediately available in PubMed Central and other publicly funded repositories, such as the WHO COVID database with rights for unrestricted research re-use and analyses in any form or by any means with acknowledgement of the original source. These permissions are granted for free by Elsevier for as long as the COVID-19 resource centre remains active.

Sustainable Cities and Society 74 (2021) 103188

Contents lists available at ScienceDirect

Sustainable Cities and Society

journal homepage: www.elsevier.com/locate/scs

Airborne infection risks of SARS-CoV-2 in U.S. schools and impacts of different intervention strategies

Yifang XU [a,*], Jiannan CAI, Ph.D. [b,*], Shuai LI, Ph.D. [a,*], Qiang HE, Ph.D. [a], Siyao ZHU [c]

[a] Department of Civil and Environmental Engineering, University of Tennessee, Knoxville. 851 Neyland Drive, Knoxville TN 37996, USA
[b] Department of Construction Science, The University of Texas at San Antonio. 501 W César E Chávez Blvd, San Antonio, TX 78207, USA
[c] Department of Civil and Systems Engineering, Johns Hopkins University, Baltimore. 3400 N. Charles St., Baltimore, MD 21218, USA

ARTICLE INFO

Keywords:
COVID-19
Airborne infection risks
Intervention strategies
Schools
Policy

ABSTRACT

The potential airborne transmission of SARS-CoV-2 has triggered concerns as schools continue to reopen and resume in-person instruction during the current COVID-19 pandemic. It is critical to understand the risks of airborne SARS-CoV-2 transmission under different epidemiological scenarios and operation strategies for schools to make informed decisions to mitigate infection risk. Through scenario-based analysis, this study estimates the airborne infection risk of SARS-CoV-2 in 111,485 U.S. public and private schools and evaluates the impacts of different intervention strategies, including increased ventilation, air filtration, and hybrid learning. Schools in more than 90% of counties exhibit infection risk of higher than 1%, indicating the significance of implementing intervention strategies. Among the considered strategies, air filtration is found to be most effective: the school average infection risk when applying MERV 13 is over 30% less than the risk levels correlating with the use of increased ventilation and hybrid learning strategies, respectively. For most schools, it is necessary to adopt combined intervention strategies to ensure the infection risk below 1%. The results provide insights into airborne infection risk in schools under various scenarios and may guide schools and policymakers in developing effective operations strategies to maintain environmental health.

1. Introduction

Severe acute respiratory syndrome coronavirus 2 (SARS-CoV-2) is identified as the virus that causes the coronavirus disease 2019 (COVID-19). The outbreak of COVID-19 spreads over 220 countries and territories (JHU, 2021), causing global pandemic and threatening human life, which reveals the urge of improving human health as an important goal of sustainability development (Hakovirta & Denuwara, 2020). Schools are considered high-risk environments for the transmission of infectious diseases due to the close and frequent contact and communication that occur among students and teachers. The negative impacts of crowded and poorly-ventilated indoor environments further raise concerns about the student health in schools.

The COVID-19 pandemic has resulted in the enactment of social distancing policies, with school closures existing among the first actions taken by governments worldwide. In the United States, prolonged school closures have affected about 55 million students enrolled in more than 130,000 K–12 schools and their parents in the U.S. (CDC, 2014), impacting their mental and physical health as well as education due to the variable efficiency of remote learning and by placing additional childcare burdens on their parents. At this stage in the pandemic, which is marked by increasing vaccine rollout, many schools in the U.S. are considering reopening or have already reopened for in-person instruction. However, concerns persist as the chance of contracting and transmitting COVID-19 increases in crowded indoor environments. Although several studies have indicated that children are less susceptible to experiencing severe COVID-19 (Yuki et al., 2020; Lee et al., 2020), those with mild or asymptomatic cases without confirmed diagnoses and treatment may facilitate rapid transmission of the disease within schools and to households and the surrounding communities. So far, it is not recommended for K–12 schools to screen all students for symptoms of COVID-19 on a routine basis (CDC 2021a), which poses a potential risk for the spread and outbreak of the disease within schools. In addition, no vaccines have yet been approved for children and, even in vaccinated people, the risk of SARS-CoV-2 infection is not entirely eliminated (CDC, 2021b). Due to the important role of schools in children's growth and the high prevalence of COVID-19 across the U.S., non-pharmacological interventions are required to help limit the spread of COVID-19 and other respiratory illnesses and maintain a healthy

* Corresponding author
E-mail addresses: yxu79@vols.utk.edu (Y. XU), jiannan.cai@utsa.edu (J. CAI), sli48@utk.edu (S. LI), qianghe@utk.edu (Q. HE), szhu34@jhu.edu (S. ZHU).

https://doi.org/10.1016/j.scs.2021.103188
Received 14 April 2021; Received in revised form 30 June 2021; Accepted 15 July 2021
Available online 20 July 2021
2210-6707/© 2021 Elsevier Ltd. All rights reserved.

Nomenclature

ρ	ratio of true infections to confirmed cases
d_c	number of days from February 12, 2020 to the current date
IR	probability of susceptible individuals becoming infected
I	number of infectors
V	room volume (m^3)
N	total disinfection rate of the environment (hr^{-1})
t	exposure duration of susceptible individuals to infectors (h)
p	pulmonary ventilation rate (m^3 /h)
φ	quantum generation rate (quanta/h)
c_v	viral load in the sputum (RNA copies/mL)
c_i	conversion factor
p	standardized daily test-positivity rate
D	droplet diameter (cm)
V_d	volume of a droplet (cm^3)
N_d	droplet concentration ($\#/cm^3$)
$\lambda_{ventilation}$	outdoor ventilation rate (hr^{-1})
$k_{filtration}$	particle removal rate due to filtration (hr^{-1})
$\lambda_{recirculated}$	recirculation rate (hr^{-1})
η_{filter}	filtration efficiency

environment in schools.

Several studies have demonstrated that SARS-CoV-2, like other respiratory viruses (e.g., influenza, tuberculosis, and measles (Ather et al., 2021), can be transmitted by way of an airborne route (Morawska & Cao, 2020; Setti et al., 2020), wherein the infectious aerosols are dispensed and suspended over long distances in the air, and inhaled by the susceptible individuals (WHO, 2021). The spread of airborne diseases indicates the significance of dedensification and introducing fresh air into the crowded and poorly-ventilated buildings. For schools, dedensification can effectively help students to maintain adequate physical distancing and can be achieved by the use of hybrid learning. Meanwhile, improved ventilation and air filtration can introduce fresh air and dilute the concentration of airborne infectious particles indoors. However, the infection risks in schools of different levels (e.g., elementary vs. high schools) and how different intervention strategies quantitatively influence infection risk in different pandemic scenarios given various relevant school and disease factors (e.g., occupant density, school hours, pulmonary ventilation rate) remain elusive.

To close this gap, this study conducted scenario-based analyses to examine the relationship between the risk for airborne infection and different intervention strategies in 111,485 public and private schools in the U.S., using the COVID-19 pandemic as the epidemiological context. Specifically, two epidemiological scenarios were employed to predict both the long- and short-term risks under different intervention strategies. Monte Carlo simulation (MCS) and sensitivity analysis were also performed to exploit the impacts of various school characteristics and epidemic situation. The results provide insights for schools and governments regarding the control of infection risk using effective mitigation measures. Although this study focuses on controlling the SARS-CoV-2 infection risk in U.S. schools, the framework can be extended to other infectious diseases within other indoor environments in other countries, to maintain a healthy and sustainable environment.

2. Data and methods

2.1. Data description

A total of 111,485 schools in the U.S., including 90,160 public schools and 21,325 private schools, were analyzed in this study. Basic information about schools was retrieved from the National Center for Education Statistics (NCES, 2021), including school type, school level, school location, and total numbers of students and teachers. Schools were divided into public schools and private schools and, based on the lowest and highest grades offered, stratified as follows: pre-kindergarten, elementary, middle, high, and secondary schools for public schools and elementary, secondary, and combined schools for private schools, respectively. The school population was determined as the sum of students and full-time–equivalent teachers.

To assess the airborne infection risk in schools, the occupant density of school buildings was estimated from 1,433 representative schools across different levels. The representative schools with clear building characteristics shown in Google Maps (Google, LLC, Mountain View, CA, USA) were selected from the aforementioned 111,485 schools to retrieve the gross floor area. To reduce human errors in acquiring the gross floor area of the representative schools, a standard process was designed and followed: 1) the schools were observed using Google Maps street view to ensure that the building boundaries, the number of buildings, and the number of floors of each building can be clearly recognized; 2) For the buildings that were clearly recognized, the building area was manually collected using the area calculator tool in the Google Maps API by drawing an enclosed line along the building boundary; 3) A total of 1,433 schools were finally selected to calculate the gross floor area. The gross floor area of each school building was computed as the product of the building area and number of floors; The gross floor area of the school was the sum of space of all school buildings. The occupant density of a school was computed as the ratio of school gross floor area to the school population. The mean and standard deviation values of occupant density of each school level were then estimated based on the corresponding representative schools. The relevant descriptive statistics are provided in Table 1.

2.2. Epidemiological scenarios

In this study, the following two epidemiological scenarios were considered: a one-year pandemic scenario based on long-term projections of COVID-19 prevalence and the current epidemiological scenario across the U.S. based on recorded COVID-19 infection cases to date. The one-year pandemic scenario indicated the temporal-varying prevalence, considering the seasonal variation and immunity duration of SARS-COV-2, and was used to provide insights into long-term strategies in school operations by estimating the general trend of infection risk in schools. Separately, the current epidemiological scenario demonstrated the county-level prevalence based on the records of confirmed cases and was used to provide guidance for timely adjustment of school operations based on local conditions.

2.2.1. One-year pandemic scenario

The long-term projection model developed in the study by Kissler et al. (2020) was adopted to estimate the nationwide prevalence of SARS-CoV-2 during the post-pandemic period. The transmission dynamics of SARS-CoV-2 were determined according to seasonal variation, duration of immunity, and cross-immunity due to prior transmission of other coronaviruses (e.g., HCoV-OC43, CoV-HKU1). Seasonal variation affected the peak incidence and severity of wintertime outbreaks, while the duration of immunity and the level of cross-immunity impacted the total incidence and the pattern of recurrent circulation. Specifically, this study used a one-year pandemic scenario with moderate seasonal forcing (i.e., the R_0 in summertime is 0.8 of that in wintertime), an immunity duration of 10 weeks, and no cross-immunity between SARS-CoV-2 and other coronaviruses. The relatively short immunity duration was assumed, considering the rapid decrease of SARS-CoV-2 antibody levels and the short duration between reinfections (Edridge et al., 2020; Long et al., 2020; Iwasaki, 2020). The resulting prevalence of COVID-19 (i.e., number of infections per 1,000 people) is illustrated in Fig. 1.

Table 1
School information descriptive statistics.

School	Total Schools	Representative schools	Students		FTE teachers		Occupant density (m^2/student)	
			Mean	SD	Mean	SD	Mean	SD
All schools	111,485	1,433	427	432	30	25	14.93	5.45
Public	90,160	1,106	538	440	33	25	14.99	5.07
Private	21,325	327	192	250	16	21	14.72	6.6
PK	1,131	56	175	171	9	10	16.04	5.88
Elementary (K–5)	64,998	944	396	246	25	15	14.19	5
Middle (grades 6–8)	16,087	127	595	350	37	21	16.52	5.54
High (grades 9–12)	20,785	148	717	743	43	41	16.02	5.6
Secondary (grades 6–12)	2,475	72	306	351	26	26	17.39	6.19
Combined (PK–12)	6,009	86	242	356	24	31	15.9	7.07

FTE: full-time–equivalent; PK: pre-kindergarten; SD: standard deviation

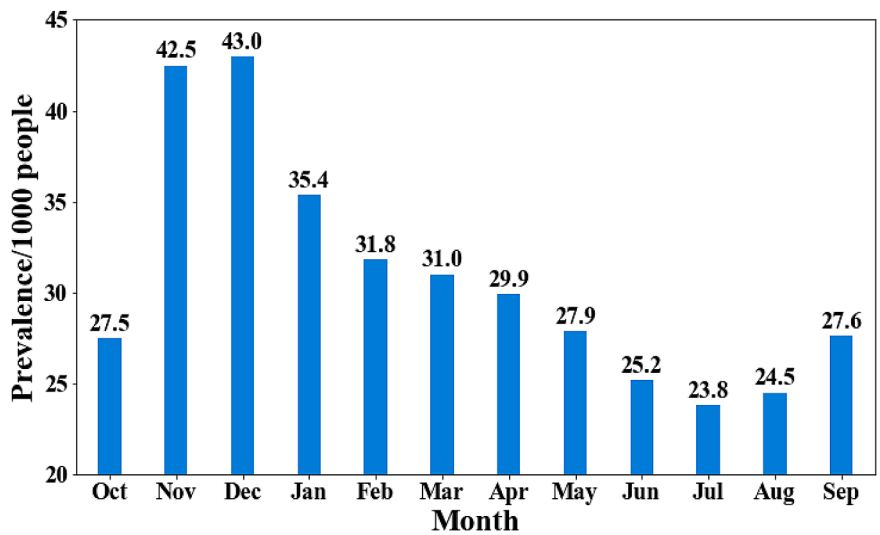

Fig. 1. Prevalence of COVID-19 in the population (generated based on Kissler et al. (2020)).

2.2.2. Current epidemiological scenario across the U.S

Identifying the COVID-19 infection rate in local areas is critical to understand the current epidemiological scenario and develop corresponding intervention strategies to mitigate infection risk in schools. However, the true number of infections is typically underestimated because a large proportion of infected individuals—especially those who are asymptomatic or only mildly symptomatic—develop the disease without a confirmed diagnosis. A study from the University of Texas at Austin (Fox, Lachmann, & Meyers, 2020) indicated that the reported cases should be multiplied by 3 to 10 as the lower and upper estimate of true infections. The Centers for Disease Control and Prevention (CDC) stated that approximately 1 in 4.3 total infection cases nationwide were reported (CDC, 2021c). In this study, the true number of current infection cases in each county was estimated based on the method developed by Gu (2021), where the relationship between the ratio of true infections to confirmed cases and the standardized test positivity rate can be computed using Equation 1:

$$\boldsymbol{\rho} = \frac{1500}{\mathbf{d_c} + 50}\mathbf{r}^{0.5} + 2 \tag{1}$$

where $\boldsymbol{\rho}$ is the ratio of true infections to confirmed cases; $\mathbf{d_c}$ is the number of days from February 12, 2020 to the current date; and $\mathbf{r}$ is the standardized daily test-positivity rate. The model standardizes the test-positivity rate across all states in the U.S. due to differences in the criteria and units of test reports. Most states use "test encounters" (TE) or "test specimens" (TS) to report test totals, but nine states use "unique individuals" (UI). TE, TS, and UI are three ways of counting the number of total tests. TE or TS is the number of people or specimens been tested per day, including the multiple tests on the same person. UI is the number of individuals being tested during the reporting period, with multiple tests on the same person removed. In (Gu, 2020), TE and TS results are treated as equivalent units, while UI results are converted to TE or TS values. The unit conversion factor ($\boldsymbol{\alpha_m}$) was estimated as the daily average ratio of daily test totals, reported as TE or TS, to those reported as UI of states that provide data using both units (e.g., TE and UI or TS and UI). The adjusted daily TE or TS test total is the product of $\boldsymbol{\alpha_m}$ and the test total reported as UI. The daily standardized test-positivity rate can be determined with the state-adjusted test total. The parameters in Eq. (1) are determined through curve-fitting on historical test positivity, serological surveys, and hospitalization data, where the constants are estimated using grid search. The true number of people becoming infected is the product of daily confirmed cases and $\boldsymbol{\rho}$, and the county infection rate is computed as the true number of infections divided by the county population size.

2.3. Infection risk modeling

With a focus on airborne transmission, infection risk in this study was defined as the probability that susceptible individuals will be infected via airborne transmission after one day of in-person school attendance. Infection risk was calculated using the Gammaitoni–Nucci (G-N) equation, a widely adopted method (Gammaitoni & Nucci, 1997) for indoor airborne infection risk assessment (e.g., influenza, tuberculosis, SARS-CoV-2). The G-N equation is a variation of an earlier model proposed by Wells-Riley et al. (W-R equation) (Riley et al., 1978); this latter

equation is based on the concept of the "quantum of infection," according to which the probability of infection is determined by the intake dose of airborne pathogens in terms of the number of quanta. Randomly distributed infectious particles in the air are considered to follow a Poisson distribution. The assumption of a steady-state particle concentration is the main limitation of the W-R equation. To overcome this limitation, the G-N equation demonstrates concentration changes in quanta level using a differential equation and considers the time-weighted average pathogen concentration rather than assuming the steady-state concentration (Sze To & Chao, 2010). In the G-N equation, the probability of susceptible individuals becoming infected (**IR**) after a certain duration of exposure can be calculated using Eq. (2) (Beggs et al., 2010; Hota et al., 2020; Buonanno et al., 2020a), where **I** is the number of infectors, **V** is the room volume ($\mathbf{m}^3$), **N** is the total disinfection rate of the environment ($\mathbf{hr}^{-1}$), **t** is the exposure duration of susceptible individuals to infectors (h), **p** is the pulmonary ventilation rate ($\mathbf{m}^3/\mathbf{h}$), and $\boldsymbol{\varphi}$ is the quantum generation rate (quanta/h).

$$\mathbf{IR} = 1 - \mathbf{e}^{-\frac{\mathbf{pI}\varphi}{\mathbf{V}}\left(\frac{\mathbf{Nt}+\mathbf{e}^{-\mathbf{Nt}}-1}{\mathbf{N}^2}\right)} \tag{2}$$

In this study, I was calculated differently according to the two epidemiological scenarios. In the one-year pandemic scenario, I was estimated as the product of the school population and the prevalence of COVID-19 in the population divided by 1,000 (note the prevalence of COVID-19 is the number of positive cases per 1,000 people in the one-year pandemic scenario). In the current epidemiological scenario, I was the product of the county infection rate and school population. V was estimated as the product of the occupant density, school population, and the height of the classroom, where a height of 3 m was assumed for all schools (DOE, 2009). t was set as the number of hours in a typical school day, varying across different states according to (NCES, 2008). N is the effect of introducing and circulating fresh air in the building. In this study, a ventilation rate of 2 $\mathbf{hr}^{-1}$ was set as the baseline rate (Batterman et al., 2017). Because **p** varies with different age groups (EPA, 2011), different values were assigned to each school level (Table 2), and $\boldsymbol{\varphi}$ for SARS-CoV-2 was estimated as a function of **p** using Eq. (3) as follows according to (G. Buonanno et al., 2020b):

$$\boldsymbol{\varphi} = \mathbf{c_v c_i p}\left(\sum_{\mathbf{i}=1}^{4} \mathbf{V_{d,i} N_{d,i,j}}\right) \tag{3}$$

where $\mathbf{c_v}$ is the SARS-CoV-2 viral load in the sputum, set at 10^9 RNA virus copies $\mathbf{mL}^{-1}$ (G. Buonanno et al., 2020b); $\mathbf{c_i}$ is a conversion factor between the infectious quantum and infectious dose, set as 0.02 (G. Buonanno et al., 2020b); **p** is the pulmonary ventilation rate based on school level ($\mathbf{m}^3/\mathbf{h}$); $\mathbf{V_{d,i}}$ is the volume of a droplet calculated by the droplet diameter $\mathbf{D_i}$; and $\mathbf{N_{d,i,j}}$ is the droplet concentration per $\mathbf{cm}^3$ of droplet diameter **i** and expiratory activity **j** (see Table 3 for details). Since the quantum generation rate is related with the degree of infection, the individual difference of pulmonary ventilation rate, the activity the patient involved in, and the range of the quantum generation rate of SARS-CoV-2 varies in the literatures. The quantum generation rate for different school levels is in accordance with recent studies. Shen et al. (2021) indicated that the quantum generation rate for children under 16 is 58 ± 31 $\mathbf{h}^{-1}$; The quantum generation rate used in Buonanno et al. (2020b) is 142 $\mathbf{h}^{-1}$ for subjects performing speaking and light activity. The estimated quantum generation rate in Dai and Zhao (2020) is 14–48 $\mathbf{h}^{-1}$. Generally, the quantum generation rates are from tens to hundreds in the literatures. In this paper, the quantum generation rate is set as 31.16, 42.72, and 51.94 $\mathbf{h}^{-1}$ for prekindergarten, elementary and combined school students respectively, and is 61.16 $\mathbf{h}^{-1}$ for middle, high, and secondary school students.

Table 3
Droplet concentration (per $\mathbf{cm}^3$) of different droplet size distributions during speaking activity (adapted from Buonanno et al., 2020b).

Expiratory activity	$\mathbf{D_1}$ (0.8 μm)	$\mathbf{D_2}$ (1.8 μm)	$\mathbf{D_3}$ (3.5 μm)	$\mathbf{D_4}$ (5.5 μm)
Voiced counting	0.236	0.068	0.007	0.011
Unmodulated vocalization	0.751	0.139	0.139	0.059

Note: Regarding respiratory activity, speaking is considered the main activity during school hours and is defined as the mean value between unmodulated vocalization and voiced counting.

2.4. Modeling the impact of different intervention strategies

The impact of different intervention strategies on the airborne infection risk was modeled by modifying the parameters in Eq. (2). The considered intervention strategies included increasing the outdoor ventilation rate, implementing air filtration, adopting hybrid learning (students learning partially online), and a combination of these three strategies.

1. Increase in outdoor ventilation rate (S1). Increasing the outdoor ventilation rate will bring in more fresh outdoor air to dilute contaminated indoor air, thus reducing the infection risk. This study modeled the impact of increasing the baseline ventilation rate by various levels (from 25% to 200% in steps of 25%) on the infection risk.
2. Implementation of air filtration (S2). When filtration is applied in a building's heating, ventilation, and air conditioning (HVAC) system, the total disinfection rate of the environment (N) can be modeled as a combined effect of outdoor ventilation and filtration, computed as $\mathbf{N} = \boldsymbol{\lambda}_{\mathbf{ventilation}} + \mathbf{k}_{\mathbf{filtration}}$, where $\mathbf{k}_{\mathbf{filtration}}$ is the particle removal rate due to filtration (Hota et al., 2020), which can be calculated using Eq. (4) (Azimi & Stephens, 2013) as follows:

$$\mathbf{k}_{\mathbf{filtration}} = \boldsymbol{\lambda}_{\mathbf{recirculated}}\boldsymbol{\eta}_{\mathbf{filter}} \tag{4}$$

where $\boldsymbol{\lambda}_{\mathbf{recirculated}}$ is the recirculation rate, set as 6.4 $\mathbf{hr}^{-1}$ (Chan et al., 2016), and $\boldsymbol{\eta}_{\mathbf{filter}}$ is the filtration efficiency weighted by infectious particle size. American Society of Heating, Refrigerating and Air-Conditioning Engineers (ASHRAE) specifies the method by which to determine $\boldsymbol{\eta}_{\mathbf{filter}}$ based on the minimum efficiency reporting value (MERV) and particle size range (ASHRAE Standard 52.2-2017) and has suggested that filters with MERVs of at least 13 can efficiently capture airborne viruses (ASHRAE, 2020). Therefore, the impact of adopting MERV 13 filters is estimated in this paper. The filtration efficiency of MERV 13 filters is 67.5% based on the assumed particle size range of SARS-CoV-2. (Morawska et al., 2020) indicates that more than half of the viral RNA of SARS-CoV-2 have aerosols smaller than 2.5 μm. In this study, it is assumed that half of the particles are 0.3 to 1 μm in size (50% average particle size efficiency) and the other half are 1 to 3 μm (85% average particle size

Table 2
Pulmonary ventilation rate of each school level based on student age groups.

Parameter	PK	Elementary	Middle	High	Secondary	Combined	Reference
Age (years)	3–5	5–11	11–14	14–18	11–18	3–18	NCES
Pulmonary ventilation rate (m^3/day)	7.28	9.98	14.29	14.29	14.29	12.135	Literature (EPA, 2011)

NCES: National Center for Education Statistics; PK: pre-kindergarten

efficiency).

3. Hybrid learning (S3). Having part of the student body learn online reduces the school population and thus decreases the number of infectors (**I**) given the specific prevalence of COVID-19 estimated from two epidemiological scenarios. In this paper, the impact of switching 10%, 20%, 30%, 40%, and 50% of the students to online learning, respectively, was computed.

4. Combined strategies. The impacts of different combinations of strategies—including increasing the ventilation rate and implementing filters (S1 + S2, denoted as S4; increasing the ventilation rate and switching part of the student body to online learning (S2 + S3, denoted as S5); and increasing the ventilation rate, implementing filtration, and switching part of the student body to online learning (S1 + S2 + S3, denoted as S6)—were considered.

2.5. Modeling the impact of parameter uncertainties

The risk of COVID-19 infection in schools may vary due to the uncertainty of multiple parameters, such as occupant density, pulmonary ventilation rate, and exposure duration. In this study, MCS and sensitivity analysis were used to quantify the influence of uncertainties of multiple parameters.

2.5.1. MCS

MCS is a method widely used to calculate possible outcomes as well as the associated uncertainty using multiple variables with different probability distributions. Based on Eq. (2), a stochastic MCS was developed to represent the uncertainty of infection risk. MCS demonstrates the uncertainty and stochasticity of the factors, and the outcomes reveal the possible results with a large variation, indicating both average and extreme case scenarios of school infection risk (Karsten et al. 2005). In this study, the MCS contained three steps: random variable determination, random number generation, and simulation result acquisition.

1 Random variable determination. Three parameters with uncertainties that will influence infection risk in schools were treated as random variables, including occupant density, pulmonary ventilation rate, and exposure duration in a school day. The possible range and empirical probability distribution of each variable were estimated based on school information and existing literature and are detailed in Table 4.

2 Infection risk simulation. Given a specific ventilation rate, 10,000 simulations were conducted to estimate the school infection risk. In each simulation, a random number was generated using repeated random sampling from the empirical distributions of each input variable and used to compute the infection risk of all schools. In this study, 10,000 simulations were performed under a ventilation rate varying from 2 to 6 hr^{-1}. Specifically, the peak prevalence of COVID-19 in the one-year pandemic scenario was used when calculating the infection risk.

3 Simulation result acquisition. For each school, 10,000 simulation results could be achieved using Eq. (2). For each simulation, the average infection risk was computed among all schools. The obtained result of 10,000 simulations indicates the distribution of average infection risk of schools nationwide.

2.5.2. Sensitivity analysis

Sensitivity analysis was conducted to evaluate the influence of individual parameters, including infection rate, exposure time, occupant density, and pulmonary ventilation rate. The estimated ranges and default values of the parameters are listed in Table 5. The infection rate was determined based on the current epidemiological scenario across the U.S. and ranged from 50% of the minimum estimated infection rate to 150% of the maximum estimated infection rate as of January 30, 2021. The pulmonary ventilation rate used in the sensitivity analysis was the average pulmonary ventilation rate of elementary school students (aged 6–11 years), because elementary schools account for more than 50% of the total number of schools nationwide.

3. Results

3.1. Infection risks under the one-year pandemic scenario

Adopting the one-year pandemic scenario (Kissler et al., 2020), the infection risk of SARS-CoV-2 in 111,485 U.S. schools was estimated for a 12-month period and reported per month in Fig. 2. A ventilation rate of two air changes per hour (ACH) in schools (Batterman et al., 2017) was used as the baseline to represent normal ventilation operation. The daily infection risk was derived based on the exposure time for each single school day, and was considered to remain unchanged within a single month. The average infection risks in schools exhibit strong patterns of seasonality, reaching a peak in winter months and a trough in summer months (e.g., the school average infection risk reaches 6.83% in December and drops to 3.85% in July), suggesting that adaptive measures could be implemented as a function of the seasonal risk to control infection. The prediction of a greater prevalence of COVID-19 (i.e., number of cases per 1,000 people) from November to February (Fig. 1) indicates a higher number of infectious students attending schools, elevating the infection risk. High schools exhibit the greatest average infection risk, followed by middle and secondary schools, while the infection risk in pre-kindergarten and elementary schools remains lower. Infection risk is largely affected by human pulmonary ventilation rate, which determines the amount of virus in aerosols exhaled by infectious people and inhaled by susceptible people. The pulmonary ventilation rate of teenagers (14.29 m^3/day) is almost twice that of younger children (7.28 m^3/day) (EPA, 2011). Thus, with the same baseline ventilation and similar occupant density, middle and high schools would have higher risks than pre-kindergarten and elementary schools. The differences among schools in terms of infection risk suggest that time-varying intervention strategies could be adopted according to a school's risk level and characteristics.

Table 5
Parameters used in the sensitivity analysis.

Parameter	Max.	Min.	Default value	Reference
Infection rate (%)	48.9	0	2.18	Literature (Gu 2021)
Exposure time (h)	7.08	6.25	6.67	NCES, 2008
Occupant density(m^2/people)	3.48	37.75	14.93	Table 1
Pulmonary ventilation rate (m^3/day)	19.02	5.29	9.98	Literature (EPA, 2011)

Table 4
Random variables used in MCS.

Parameter	PK	Elementary	Middle	High	Secondary	Combined	Distribution	Reference
Occupant density (m^2/people)	5.34–27.97	3.49–28.82	6.76– 28.92	6.38– 29.26	4.08– 28.64	4.03– 37.75	Truncated normal	Table 1
Pulmonary ventilation rate(m^3/day)	5.29– 9.27	7.11–12.85	9.56– 19.02	9.56– 19.02	9.56– 19.02	9.37–14.9	Truncated normal	Literature (EPA, 2011)
School day (hrs/day)	6.25–7.08						Truncated normal	NCES, 2008

NCES: National Center for Education Statistics; PK: pre-kindergarten

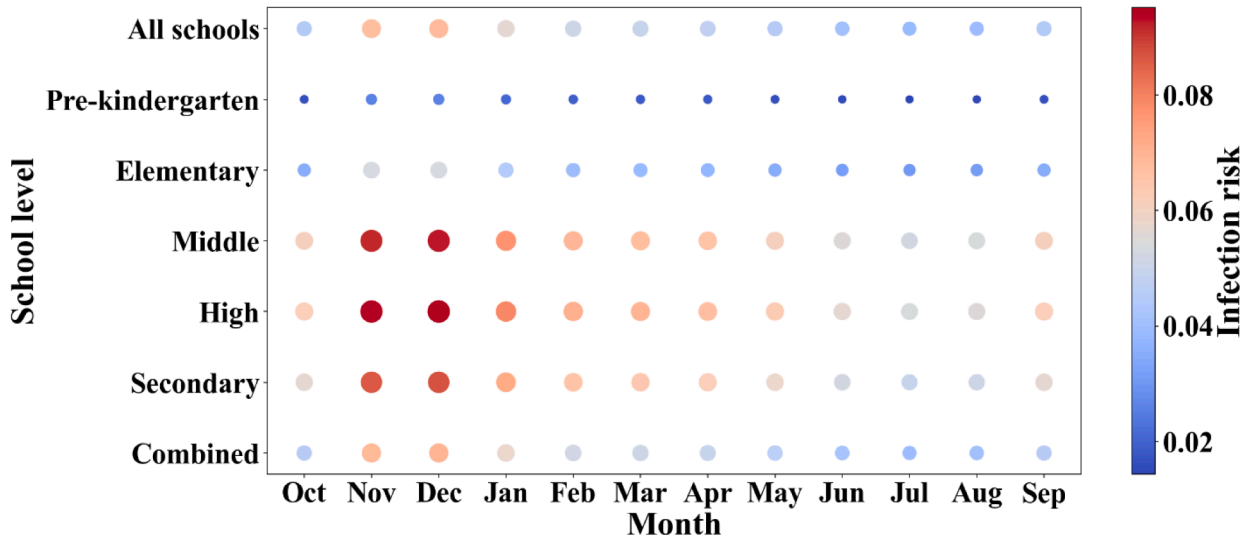

Fig. 2. Monthly average infection risk with normal school operation.

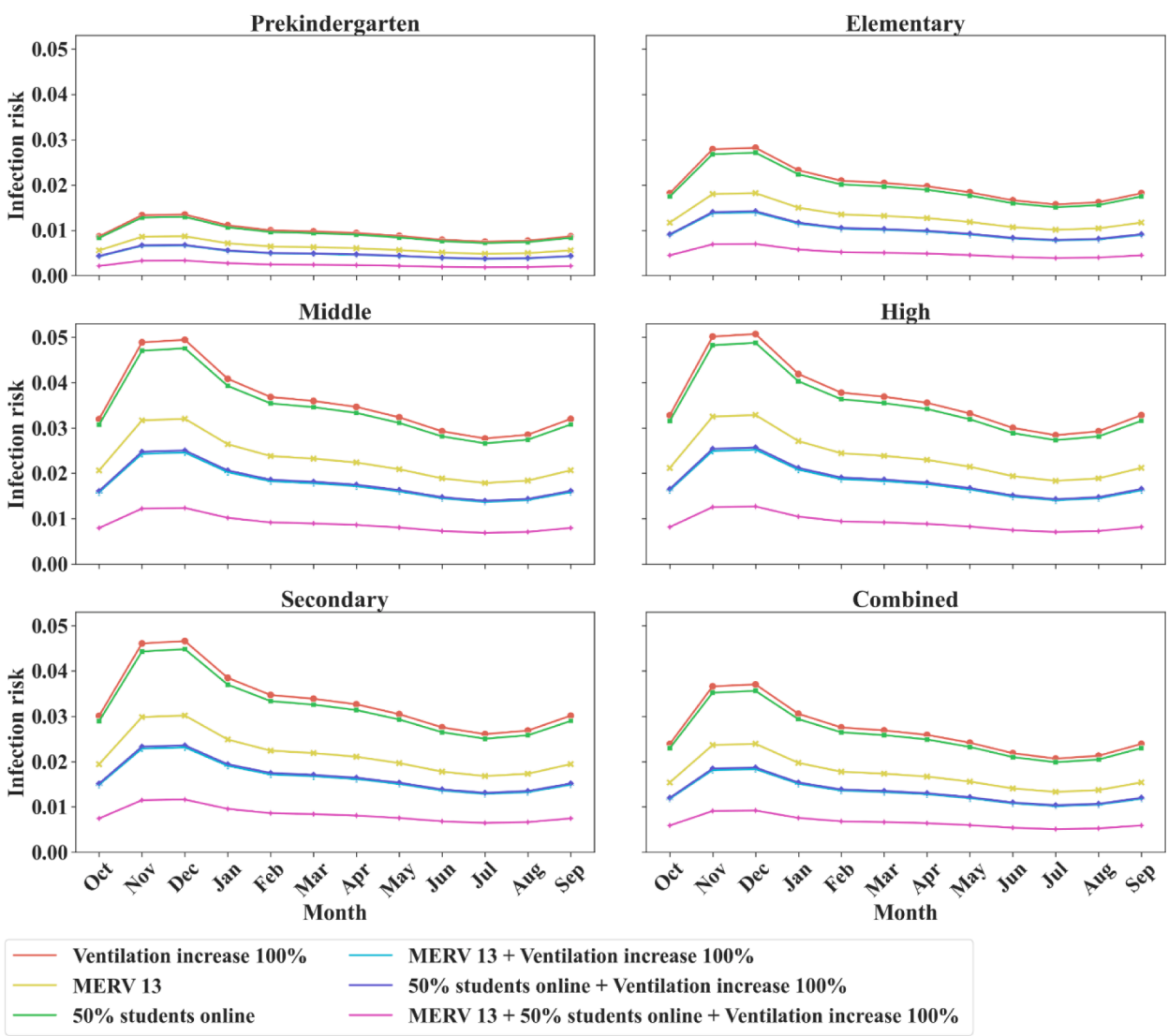

Fig. 3. Monthly average infection risk under different intervention strategies.

Different intervention strategies have different impacts on the infection risk (Fig. 3). The results illustrate that, among the three basic intervention strategies—increasing the ventilation rate by 100% (S1), implementing MERV 13 filters (S2), and having half of the student body learn online (S3)—the infection risk under S3 is slightly lower than that under S1, while S2 is the most effective strategy and results in a significantly reduced infection risk relative to both S1 and S3. Among all schools, pre-kindergarten maintains the lowest average infection risk throughout the year, which can be controlled below a sufficiently low threshold (1% in this study) solely by implementing S2. In contrast, for the other school levels, combined intervention strategies are required to keep the infection risk below 1% throughout the year. The considered combined intervention strategies include the combination of S1 and S2 (denoted as S4), the combination of S1 and S3 (denoted as S5), and the combination of S1 through S3 (denoted as S6). It was observed that the effects of S4 and S5 are almost the same, indicating that, if MERV 13 filters are not compatible with the existing HVAC system, schools may have to consider S5 to achieve a similar degree of infection risk reduction. By implementing S6, elementary and combined schools can keep the infection risk below 1% throughout the year. However, in middle, high, and secondary schools, the infection risk may exceed 1% during wintertime, where more restrictive measures (e.g., further increasing the ventilation rate, implementing filters with a higher MERV rating, and increasing the proportion of students enrolled in online learning) may be necessary to maintain the infection risk at a sufficiently low level. Given the varying prevalence throughout the year, schools may select different strategies to ensure an acceptable risk while considering other factors, such as energy costs and learning outcomes.

Fig. 4 presents the distribution of infection risk under various ventilation rates obtained using MCS. The results illustrate that the variation of infection risk decreases as the ventilation rate increases. For schools with the baseline ventilation rate (2 hr^{-1}), the mean infection risk is around 7% and the highest infection risk is 10%, demonstrating a high level of uncertainty and the significance of adopting intervention strategies. The efficiency of increasing the ventilation rate decreases as the ventilation rate increases: the infection risk decreases by 16.5% when the ventilation rate is increased from 2 hr^{-1} to 2.5 hr^{-1}, while it only decreases by 8% when the ventilation rate is increased from 5.5 hr^{-1} to 6 hr^{-1}. Therefore, to further reduce the infection risk, increasing the ventilation rate alone may not be the most efficient strategy when considering the energy required. Schools might also contemplate adopting complementary mitigation measures to maintain low infection risk levels and energy costs.

3.2. Infection risks under the current epidemiological scenario

The infection risk for each state under different intervention strategies is presented in Fig. 5. The average infection risk of a state is computed as the mean value of the infection risks over all counties in the state, and the range of the infection risk of a state is represented as the range of the infection risk of the counties with 95% confidence interval. The infection risk for each county is computed based on county epidemic situation and the characteristics of schools in the county. For most states, schools with the baseline ventilation rate show a high infection risk, with an average infection risk of 3.75%. Under the current epidemiological scenario, more than 90% of counties exhibit an infection risk of greater than 1%, indicating the significance of implementing intervention strategies to decrease the infection risk. The impacts of increasing the ventilation rate by 100% (S1) and having half of students learn online (S3) are similar, resulting in average infection risks of 1.98% and 1.90%, respectively. Under both strategies, the infection risk of nearly 20% of counties nationwide falls below 1%. Implementing MERV 13 filters (S2) outperforms both S1 and S3, with an average infection risk of 1.28%—35% and 33% lower than the infection risks calculated under S1 and S3, respectively—resulting in an infection risk below 1% for approximately 40% of counties nationwide.

The average infection risk of a given county is determined by the infection rate and the characteristics of the schools in that county. Counties with higher prevalence rates generally exhibit greater infection risk in schools. Fig. 5 shows that schools in the southeastern and southwestern U.S. are exposed to higher infection risks. Specifically, Arizona, South Carolina, Oklahoma, Mississippi, and Georgia are the five states with the highest infection rates ($\geq$ 3.18%), and the schools in these states also have the highest levels of infection risk ($\geq$ 5.5%). In addition, the infection risk in each county is also influenced by the characteristics of individual schools, especially the school level, which determines the school occupant density and the student pulmonary ventilation rate. Table 6 shows that the distribution of schools is similar across different states, indicating that a state's average infection risk depends crucially upon the infection rate. However, as shown in Table 6, the county-level school distribution varies significantly, especially for elementary and high schools, demonstrating that, in addition to the county infection rate, school distribution contributes to the variation in infection risk. These results suggest that schools and policymakers should consider and adopt specific intervention strategies based on various factors, including the local epidemic situation, school characteristics, and school HVAC system conditions. S2 is cost-effective and efficient at reducing infection risks. If MERV 13 filters are not accommodated in the school HVAC system, S1 and S2 can be used, and further increases in ventilation or in the proportion of hybrid learning may be

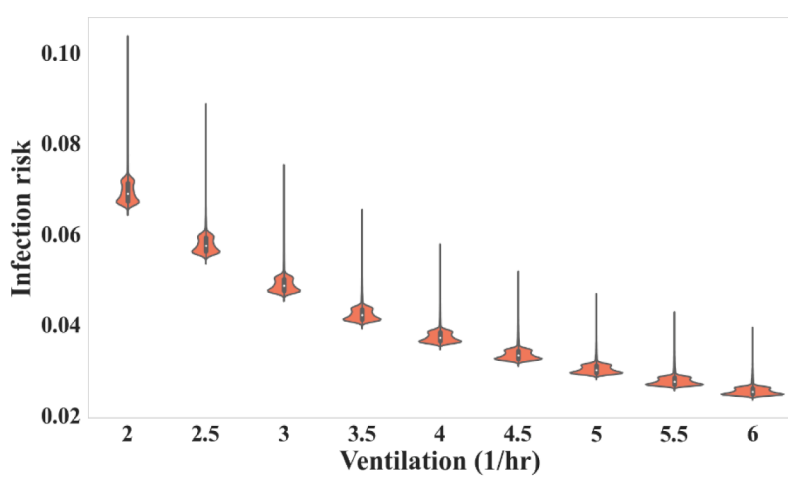

Fig. 4. Distribution of average school infection risk under various ventilation rates.

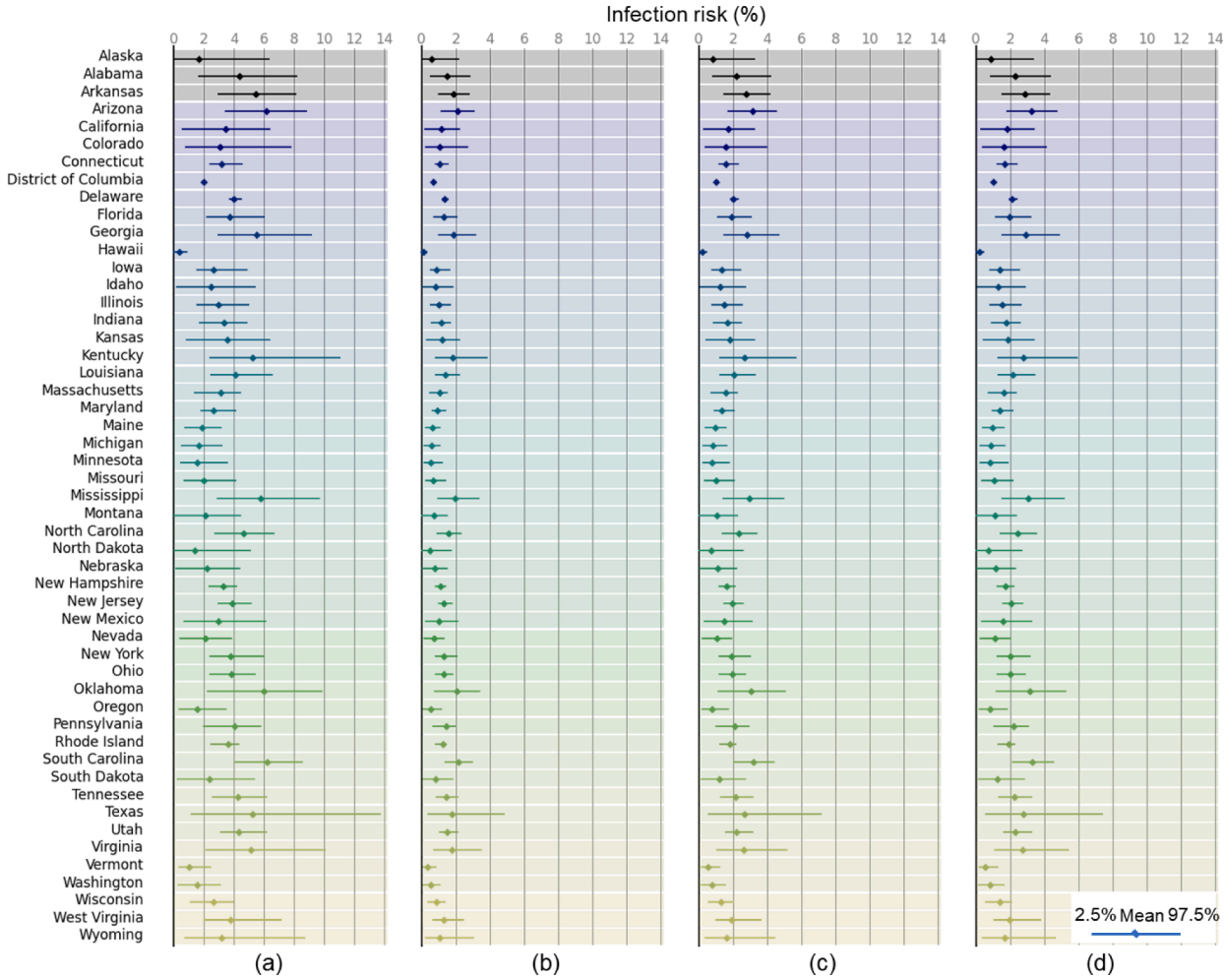

Fig. 5. Infection risk for each state with different intervention strategies: (a) the baseline scenario; (b) with MERV 13 filtration; (c) with 50% of students learning online; and (d) when increasing the ventilation rate by 100%.

Table 6
School distribution by state and county.

School level	Max.		Min.		Mean		SD	
	State	County	State	County	State	County	State	County
PK	5.13%	40%	0.00%	0%	1.11%	1.04%	0.011	0.032
Elementary	67.76%	100%	49.67%	0%	58.15%	51.61%	0.039	0.118
Middle	24.73%	50%	7.10%	0%	14.47%	15.71%	0.030	0.089
High	31.21%	100%	11.02%	0%	18.73%	25.63%	0.042	0.113
Secondary	5.46%	100%	0.53%	0%	2.18%	1.37%	0.011	0.037
Combined	14.07%	100%	1.97%	0%	5.36%	4.64%	0.026	0.071

PK: pre-kindergarten; SD: standard deviation

adopted according to the infection risk, school system capacity, and teaching quality.

3.3. Sensitivity analysis

In addition to different intervention strategies, the infection risk in schools is also sensitive to changes in multiple factors, including the infection rate of the population, exposure time in schools, occupant density, and the students' pulmonary ventilation rate. In this study, a sensitivity analysis was conducted to quantify the influence of these factors given the estimated ranges detailed in Table 5; the results of this analysis are shown in Fig. 6. The infection risk shows a near-linear relationship with the exposure time. The change in exposure time within the estimated range has a limited impact on infection risk because the average number of hours in the school day do not vary distinctly across the U.S. The infection risk increases with an increase in the infection rate parameter. The infection rate varies significantly across counties, leading to great changes in school infection risks. For instance, Forest County, Pennsylvania, exhibits the highest infection rate among all counties of 32.6% and a county infection risk of 32.9%, whereas the average infection risk for all counties nationwide is only 3.8%. Schools located in counties with high infection rates are expected to be exposed to greater risk levels and will need to adopt much stricter mitigation measures to effectively control the infection risk. Considering occupant density, the results show a sharp decrease in the infection risk, with the parameter changing from 3 to 10 square meters per student; the

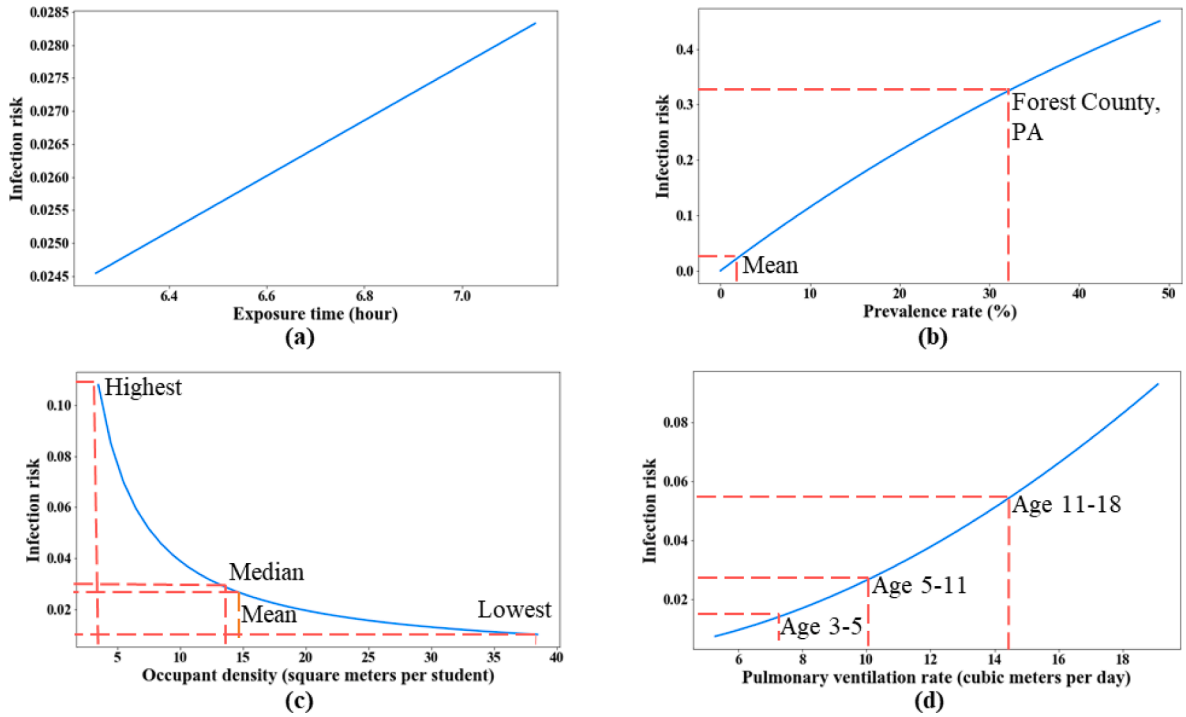

Fig. 6. Sensitivity analysis of parameters: (a) exposure time; (b) infection rate; (c) occupant density; and (d) pulmonary ventilation rate.

trend then flattens after this point. Nationwide, the infection risk reaches 10.8% for schools with the highest occupant density, while the lowest value is 1%. The mean and median values are close, and the infection risk is 2.6% with a mean value of 14.93 and 2.8% with a median value of 14.04, respectively. These results indicate that, for most schools, the current occupant density is appropriate, and further reductions in occupant density may not lead to a significantly reduced infection risk. For schools with high occupant density (e.g., 3 to 10 square meters per student), it is recommended that the density be reduced to the average level (e.g., 14.93 square meters per student). The infection risk increases as the pulmonary ventilation rate rises, with the rate of change increasing as well. The annotation in red dashed lines in Fig. 6(d) indicates the mean pulmonary ventilation rates of different school levels (as shown in Table 2) and the corresponding infection risk. The infection risk is 1.4% for pre-kindergarten students (aged 3–5 years); 2.6% for elementary school students (aged 5–11 years); and 5.3% for middle, high, and secondary school students (aged 11–18 years). The pulmonary ventilation rate increases with the maturation of children, leading to an even greater infection risk. Intervention strategies are necessary for schools with higher levels of infection risk to adopt to reduce the infection risk to a sufficiently low level.

4. Discussion

COVID-19 pandemic leads to significant education crisis all over the world. The worldwide school closure has affected over 80% of total enrolled students, and half of the students in more than 200 countries have experienced partially or fully school closures (UNESCO, 2021). Long-time school closures raise public concerns about the negative impacts on children health, education, and financial burdens on the households (Van Lancker & Parolin, 2020). Therefore, as schools reopen and resume in-person instruction, effective operation strategies are essential to maintain a healthy and sustainable learning environment.

Ventilation, social distancing, and filtration are three broadly utilized strategies during the pandemic. Several studies have been dedicated to discussing the impact of these strategies in the control of COVID-19 transmission, and achieved compatible results with this paper, despite of different pandemic scenario, indoor environment, and countries considered. Sun and Zhai (2020) introduced a distance index and a ventilation index in the Wells-Riley model to compute the infection risks in buses in China. Similar to our study, their results suggest a near-linear relationship between infection risk and the exposure time and demonstrate the efficiency of increasing ventilation and reducing occupant density in mitigating the infection risk. Shen et al. (2021) discussed the effectiveness of multi-scale strategies for reducing airborne infection risk of SARS-CoV-2 using Wells-Riley model for indoor spaces, and suggested the higher efficiency of applying filters compared to solely increasing airflow rate, which aligns with our conclusion. However, in previous studies, the number of infectors were either set to be 1 for each room which is unlikely in the actual situation, or calculated using the infection rate estimated from limited sample size. To overcome the limitation, this study leveraged data-driven and scenario-based analysis to evaluate school infection risk under various intervention strategies considering both long-term and short-term realistic pandemic scenarios.

Regarding the selection of intervention strategies in this study, given the importance of in-person interaction for student learning, the intervention strategy only considers that up to 50% of students would be learning online. Considering the current condition of most school HVAC systems, although increasing room ventilation rates is efficient in reducing infection risks, the ventilation rate cannot be increased beyond the system capacity. In this paper, doubling the baseline ventilation rate was considered to ensure that the proposed strategy would be affordable for most schools. Implementing filters with higher MERV ratings (e.g., MERV 14–16) would only have a slight effect on decreasing the infection risk but would generate additional product and energy costs. For instance, the average school infection risk in December is 2.34%, 2.04%, 1.96%, and 1.85% for implementing MERV 13–16 filters, respectively. With the increase of MERV ratings, more energy is required to overcome additional pressure drop, and the purchase cost increases from $ 11 per filter for MERV 13 filters to $50, $90, $125, $150 for MERV 14–16 filters, respectively (Azimi & Stephens, 2013). Thus, implementing MERV 13 filters was adopted as filtration intervention strategy. It is found that filtration is most effective in reducing the infection risk, resulting in a

risk reduction of more than 30% relative to that achieved with either ventilation increase or hybrid learning in both considered pandemic scenarios. However, to maintain a healthy school environment, it is suggested that multiple intervention strategies be adopted simultaneously. Beside the direct impact of intervention strategies to the airborne infection risk, it has been proved that poor air quality caused by pollutants (e.g., particulate matters and volatile compounds) may lead to acceleration of the contagion of SARS-CoV-2 (Agarwal et al., 2021). The intervention strategies can also improve the indoor air quality, and further reduce the transmission of SARS-CoV-2. Other technologies can be considered for sustainable building retrofitting together with the intervention strategies (e.g., natural ventilation, botanical biofilters (Irga et al., 2017; Abdo et al., 2019), passive cooling techniques (Abdo et al., 2020) to maintain healthy indoor environment and human comfort.

The infection risk may vary significantly across countries due to the differences in population size, disease prevalence, infection-hospitalization ratios, fraction of immunity, etc. However, the findings in this study can provide insights for other countries regarding the risk control during the pandemic. For instance, the effectiveness of intervention is analyzed and compared, including filtration, ventilation, and social distancing achieved by online learning, indicating that filtration strategy can be widely adopted for schools worldwide. In addition, the framework can be extended to other infectious diseases in other counties by considering specific disease characteristics and epidemic and operation scenarios.

5. Conclusion

The airborne infection risk of SARS-CoV-2 in U.S. schools has been estimated under different epidemiological scenarios. Multiple intervention strategies, including increased ventilation, air filtration, and hybrid learning, are modeled to evaluate their effectiveness in reducing the infection risk. Two epidemiological scenarios were considered, including a one-year pandemic scenario and a current epidemiological scenario. A series of findings and important insights were derived as follows, which will provide insights for schools and governments to develop guidelines on adopting appropriate intervention strategies to mitigate airborne infection risk considering epidemic situation and school characteristics.

1 The airborne infection risk in schools exhibits seasonal patterns, with the average infection risk in all schools ranging from 3.85% in the summer to 6.83% in the winter under the one-year pandemic scenario, indicating the necessity of adjusting mitigation measures over the year.
2 The effectiveness of intervention strategies varies with different school levels and pandemic periods and, thus, requires individual schools to adopt variable intervention strategies over the long term. In general, schools with higher school level experience higher risk. For instance, the infection risk in pre-kindergarten remains low throughout the year, and the implementation of MERV 13 filters can limit the infection risk to below 1%. For elementary schools, implementing all strategies are suggested in most months, while, in months with lower prevalence rates (e.g., summertime), schools can adopt fully in-person learning in concert with filtration and increased ventilation. For other school levels (e.g., middle, secondary, and high schools), the infection risk may persist above 1% in some months even after implementing all strategies. Additional mitigation measures, such as wearing masks and enacting further social distancing, are needed to ensure an acceptable risk level.
3 The relationships between infection risk and ventilation rates are depicted using Monte Carlo simulation, illustrating the efficiency of increasing the ventilation rate on reducing the infection risk and demonstrating the significance of combined intervention strategies when considering the capacity of school systems.
4 The infection risk for each state is computed based on the infection risk of the counties in the state under normal operations as well as various intervention strategies based on the current epidemiological scenario. Schools with the baseline ventilation rate show a high infection risk across the U.S., with more than 90% of the counties exhibit an infection risk of greater than 1%, indicating the necessity of intervention strategies to maintain a sustainable indoor environment. The results show that increasing the ventilation rate by 100% and having half of students learn online have similar impacts on reducing infection risks, while implementing air filtration is more efficient than either of the strategies, with over 30% less than the risk levels correlating with ventilation enhancement and hybrid learning.
5 Sensitivity analysis is conducted to further illustrate the impact of the characteristics of schools and the epidemic situation on infection risk. In general, the infection risk shows a near-linear relationship with the exposure time in schools. It is also found that the current occupant density is appropriate for most schools, while it is recommended that the density be reduced to the average level (e.g., 15 square meters per student) for schools with higher occupant density.

There remain some limitations in this paper. First, the estimated infection risk indicates the daily infection risk based on the exposure time in a single day, ignoring the effect of probability transition due to continuous exposure in schools, which may result in the underestimation of the result. Future study may consider the effect from the previous school days according to the specific schedule. Second, the model used in this study assumes that the infectious particles are well mixed throughout the whole school building, without considering the separation of rooms in the building and the separation of buildings if a school has multiple buildings. This is a simplification for national assessment of school infection risks. To accurately model the infection risk in a specific school, future research is needed to develop new simulation-based approach to incorporate detailed information of the school. Third, as a scenario-based analysis, derived results and findings regarding infection risk and intervention strategies are based on a one-year pandemic scenario and a short-term county-level epidemiological scenario, which might be different from actual situations. Leveraging the findings and insights regarding impacts of various intervention strategies on infection risk under different scenarios, schools and governments can design their own strategies based on their specific characteristics and epidemic conditions.

Declaration of Competing Interest

The authors declare no conflict of interest.

Acknowledgments

This work was supported by U.S. National Science Foundation via grants 1952140, 2026719, and 2038967.

References

Abdo, P., Huynh, B. P., Braytee, A., & Taghipour, R. (2020). An experimental investigation of the thermal effect due to discharging of phase change material in a room fitted with a windcatcher. *Sustainable Cities and Society, 61*, Article 102277. https://doi.org/10.1016/j.scs.2020.102277

Abdo, P., Huynh, B. P., Irga, P. J., & Torpy, F. R. (2019). Evaluation of air flow through an active green wall biofilter. *Urban Forestry and Urban Greening, 41*, 75–84. https://doi.org/10.1016/j.ufug.2019.03.013

Agarwal, N., Meena, C. S., Raj, B. P., Saini, L., Kumar, A., Gopalakrishnan, N., Kumar, A., Balam, N. B., Alam, T., Kapoor, N. R., & Aggarwal, V. (2021). Indoor air quality improvement in COVID-19 pandemic: Review. *Sustainable Cities and Society, 70*, Article 102942. https://doi.org/10.1016/j.scs.2021.102942

ASHRAE. (2020). Filtration /disinfection. https://www.ashrae.org/technical-resources/filtration-disinfection.

Ather, B., Mirza, T., & Edemekong, P. (2021). *Airborne precautions - StatPearls - NCBI bookshelf*. StatPearls. https://www.ncbi.nlm.nih.gov/books/NBK531468/.

Azimi, P., & Stephens, B. (2013). HVAC filtration for controlling infectious airborne disease transmission in indoor environments: Predicting risk reductions and

operational costs. *Building and Environment, 70*, 150–160. https://doi.org/10.1016/j.buildenv.2013.08.025

Batterman, S., Su, F. C., Wald, A., Watkins, F., Godwin, C., & Thun, G. (2017). Ventilation rates in recently constructed U.S. school classrooms. *Indoor Air, 27*(5), 880–890. https://doi.org/10.1111/ina.12384

Beggs, C. B., Shepherd, S. J., & Kerr, K. G. (2010). Potential for airborne transmission of infection in the waiting areas of healthcare premises: Stochastic analysis using a Monte Carlo model. *BMC Infectious Diseases, 10*, 247–247.

Buonanno, Giorgio, Morawska, L., & Stabile, L. (2020a). *Quantitative assessment of the risk of airborne transmission of SARS-CoV-2 infection: Prospective and retrospective applications*. MedRxiv.

Buonanno, G., Stabile, L., & Morawska, L. (2020b). Estimation of airborne viral emission: Quanta emission rate of SARS-CoV-2 for infection risk assessment. *Environment International, 141*, Article 105794. https://doi.org/10.1016/j.envint.2020.105794

CDC. (2014). Guidance for school administrators to help reduce the spread of seasonal influenza in K-12 schools. http://www.cdc.gov/flu/school/guidance.htm.

CDC. (2021a). Screening K-12 students for symptoms of COVID-19: Limitations and considerations. https://www.cdc.gov/coronavirus/2019-ncov/community/schools-childcare/symptom-screening.html.

CDC. (2021b). COVID-19 science brief : Background rationale and evidence for public health recommendations for fully vaccinated people. https://www.cdc.gov/coronavirus/2019-ncov/more/fully-vaccinated-people.html.

2021c CDC. (2021c). Estimated Disease Burden of COVID-19. https://www.cdc.gov/coronavirus/2019-ncov/cases-updates/burden.html Please reorder it to move it below CDC.

Chan, W. R., Parthasarathy, S., Fisk, W. J., & McKone, T. E. (2016). Estimated effect of ventilation and filtration on chronic health risks in U.S. offices, schools, and retail stores. *Indoor Air, 26*(2), 331–343. https://doi.org/10.1111/ina.12189

JHU. (2021). COVID-19 map - Johns Hopkins coronavirus resource center. (2021). https://coronavirus.jhu.edu/map.html.

Gu. (2021). COVID-19 projections using machine learning. https://covid19-projections.com/.

Dai, H., & Zhao, B. (2020). Association of the infection probability of COVID-19 with ventilation rates in confined spaces. *Building Simulation, 13*(6), 1321–1327. https://doi.org/10.1007/s12273-020-0703-5

DOE. (2009). *Building handbook*. https://www.education-ni.gov.uk/building-handbook.

Edridge, A. W. D., Kaczorowska, J., Hoste, A. C. R., Bakker, M., Klein, M., Loens, K., Jebbink, M. F., Matser, A., Kinsella, C. M., Rueda, P., Ieven, M., Goossens, H., Prins, M., Sastre, P., Deijs, M., & van der Hoek, L. (2020). Seasonal coronavirus protective immunity is short-lasting. *Nature Medicine, 26*(11), 1691–1693. https://doi.org/10.1038/s41591-020-1083-1

UNESCO, (2021). Education: From disruption to recovery. https://en.unesco.org/covid19/educationresponse#schoolclosures.

EPA. (2011). *Exposure factors handbook 2011* (Edition). Final Report.

Fox, S. J., Lachmann, M., & Meyers, L. A. (2020). Risks of COVID-19 introductions as schools reopen.

Gammaitoni, L., & Nucci, M. C. (1997). Using a mathematical model to evaluate the efficacy of TB control measures. *Emerging Infectious Diseases, 3*(3), 335–342. https://doi.org/10.3201/eid0303.970310

Hakovirta, M., & Denuwara, N. (2020). How COVID-19 redefines the concept of sustainability. *Sustainability, 12*(9), 1–4. https://ideas.repec.org/a/gam/jsusta/v12y2020i9p3727-d353926.html.

Hota, B., Stein, B., Lin, M., Tomich, A., Segreti, J., & Weinstein, R. A. (2020). *Estimate of airborne transmission of SARS-CoV-2 using real time tracking of health care workers*. medRxiv. https://doi.org/10.1101/2020.07.15.20154567. medRxivp. 2020.07.15.20154567.

Irga, P. J., Paull, N. J., Abdo, P., & Torpy, F. R. (2017). An assessment of the atmospheric particle removal efficiency of an in-room botanical biofilter system. *Building and Environment, 115*, 281–290. https://doi.org/10.1016/j.buildenv.2017.01.035

Iwasaki, A. (2020). *What reinfections mean for COVID-19*. The Lancet Infectious Diseases.

Karsten, S., Rave, G., & Krieter, J. (2005). Monte Carlo simulation of classical swine fever epidemics and control: I. General concepts and description of the model. *Veterinary Microbiology, 108*(3–4), 187–198. https://doi.org/10.1016/j.vetmic.2005.04.009

Kissler, S. M., Tedijanto, C., Goldstein, E., Grad, Y. H., & Lipsitch, M. (2020). Projecting the transmission dynamics of SARS-CoV-2 through the postpandemic period. *Science, 368*(6493), 860–868. https://doi.org/10.1126/science.abb5793

Lee, P. I., Hu, Y. L., Chen, P. Y., Huang, Y. C., & Hsueh, P. R. (2020). Are children less susceptible to COVID-19? *Journal of Microbiology, Immunology and Infection, 53*(3), 371–372. https://doi.org/10.1016/j.jmii.2020.02.011

Long, Q. X., Tang, X. J., Shi, Q. L., Li, Q., Deng, H. J., Yuan, J., Hu, J. L., Xu, W., Zhang, Y., Lv, F. J., Su, K., Zhang, F., Gong, J., Wu, B., Liu, X. M., Li, J. J., Qiu, J. F., Chen, J., & Huang, A. L. (2020). Clinical and immunological assessment of asymptomatic SARS-CoV-2 infections. *Nature Medicine, 26*(8), 1200–1204. https://doi.org/10.1038/s41591-020-0965-6

Morawska, L., & Cao, J. (2020). Airborne transmission of SARS-CoV-2: The world should face the reality. In *Environment International, 139*. Elsevier Ltd, Article 105730. https://doi.org/10.1016/j.envint.2020.105730

Morawska, L., Tang, J. W., Bahnfleth, W., Bluyssen, P. M., Boerstra, A., Buonanno, G., Cao, J., Dancer, S., Floto, A., & Franchimon, F. (2020). How can airborne transmission of COVID-19 indoors be minimised? *Environment International, 142*, Article 105832.

NCES. (2008). Average number of hours in the school day and average number of days in the school year for public schools.

NCES. (2021). National center for education statistics (NCES). https://nces.ed.gov/ccd/elsi/tablegenerator.aspx.

Riley, E. C., Murphy, G., & Riley, R. L. (1978). Airborne spread of measles in a suburban elementary school. *American Journal of Epidemiology, 107*(5), 421–432. https://doi.org/10.1093/oxfordjournals.aje.a112560

Setti, L., Passarini, F., De Gennaro, G., Barbieri, P., Perrone, M. G., Borelli, M., Palmisani, J., Di Gilio, A., Piscitelli, P., & Miani, A. (2020). Airborne transmission route of covid-19: Why 2 meters/6 feet of inter-personal distance could not be enough. In *International Journal of Environmental Research and Public Health, 17*. MDPI AG. https://doi.org/10.3390/ijerph17082932

Shen, J., Kong, M., Dong, B., Birnkrant, M. J., & Zhang, J. (2021). *A systematic approach to estimating the effectiveness of multi-scale IAQ strategies for reducing the risk of airborne infection of SARS-CoV-2* (p. 200). Building and Environment. https://doi.org/10.1016/j.buildenv.2021.107926

Standard 52.2- 2017 - American society of heating, refrigerating and air-conditioning engineers. https://ashrae.iwrapper.com/ASHRAE_PREVIEW_ONLY_STANDARDS/STD_52.2_2017.

Sun, C., & Zhai, Z. (2020). The efficacy of social distance and ventilation effectiveness in preventing COVID-19 transmission. *Sustainable Cities and Society, 62*, Article 102390. https://doi.org/10.1016/j.scs.2020.102390

Sze To, G. N., & Chao, C. Y. H. (2010). Review and comparison between the Wells–Riley and dose-response approaches to risk assessment of infectious respiratory diseases. *Indoor Air, 20*(1), 2–16.

WHO. (2021). Transmission of SARS-CoV-2: Implications for infection prevention precautions. https://www.who.int/news-room/commentaries/detail/transmission-of-sars-cov-2-implications-for-infection-prevention-precautions.

Van Lancker, W., & Parolin, Z. (2020). COVID-19, school closures, and child poverty: a social crisis in the making. In *The Lancet Public Health, 5* pp. e243–e244). Elsevier Ltd. https://doi.org/10.1016/S2468-2667(20)30084-0

Yuki, K., Fujiogi, M., & Koutsogiannaki, S. (2020). COVID-19 pathophysiology: A review. In *Clinical Immunology, 215*. Academic Press Inc, Article 108427. https://doi.org/10.1016/j.clim.2020.108427